General Disclaimer

One or more of the Following Statements may affect this Document

- This document has been reproduced from the best copy furnished by the organizational source. It is being released in the interest of making available as much information as possible.

- This document may contain data, which exceeds the sheet parameters. It was furnished in this condition by the organizational source and is the best copy available.

- This document may contain tone-on-tone or color graphs, charts and/or pictures, which have been reproduced in black and white.

- This document is paginated as submitted by the original source.

- Portions of this document are not fully legible due to the historical nature of some of the material. However, it is the best reproduction available from the original submission.

Final Report

on

Study of Glass Preforms for

Glass Fiber Optics Applications

(Study of Space Processing of Ceramic Materials)

JPL Contract No. 953842

SUNY Account No. 31-6089A

Period Covered: February 1, 1974 - October 1, 1974

by

Franklin F. Y. Wang
Department of Materials Science,
State University of New York at Stony Brook
Stony Brook, New York 11794

prepared for

Jet Propulsion Laboratory
California Institute of Technology
Pasadena, California 91103

Attention: M. H. Porter, Contract Negotiator

TABLE OF CONTENTS

ABSTRACT

This project was undertaken for a six (6) month period to study the feasibility, and the technical and economic desirability, of space processing of glass preforms for optical fiber transmission applications. The study involves and develops no new technology. Useful results were obtained, however, and they indicate that space processing can produce glass preforms of equal quality at greatly lower cost than earth bound production. It enables the production of larger diameter glass preform and thereby lowers the cost from a price of 8.471 ¢/m for earth-bound production to 1.964 ¢/m for space processing. This set of cost estimates is for any manufacturers who intend to produce glass fiber optics. Space processing can produce diameter modulation in the glass preform which promotes mode coupling and thereby lowers the dispersion. It can also modify the glass composition through the evaporative and diffusion processes and produce graded refractive index profile in the glass preform. By this means, the dispersion of the optical fiber will also be lowered. Consequently, the space processing has the possibility of producing glass preforms of better properties than earth-bound production. If the radiation effect becomes a significant factor, the present-day binary compositions of the doped SiO_2 type (doped by GeO_2 or TiO_2 and the like) may not be useful. Space processing will offer the greater possibilities of making glass preforms from two glasses with greater dissimilar physical properties. A brief summary of the state of the art in optical fiber transmission is included in the Appendix of this report. It can be seen that the space processing of glass preforms, as considered in this study, is compatible to the current practices in the field.

I. INTRODUCTION

This project was undertaken for a six (6) month period to study the feasibility, and the technical and economical desirability, of space processing of glass preforms for optical fiber transmission applications.

This item was selected for study because the demand for improved communication facilities requires optical communication systems; giant advances in the field of optical fiber transmission in the last two years render its eventual application in communication a foregone conclusion; glass preforms are compact in volume as well as in weight; and high purity glass materials are extremely expensive (for example, $154 per linear inch of a 1 inch diameter glass rod of the Suprasil W-1 grade) so as to make the additional cost of $160 per pound for the space processing transport cost a reasonable cost to carry. The former two conditions forcast a genuine market for the product in the immediate future. As it will be shown later in this report, the space processing of the glass preform will provide an inexpensive means for any manufacturers, who do not wish to make a major capital investment, to obtain glass fiber optics of their own choice. The low volume and weight of the glass preform render it especially suitable for space processing. Therefore, it can be concluded that the space processing of glass preform satisfies the economic and preliminary processing constraints.

In the following, several reasons are given which suggest that the space processing of glass preforms can produce superior products for the optical fiber transmission applications than its processing on the earth-bound facilities.

II. SUMMARY

During the six (6) month period, our approach in this project was to set up a reasonable premise as a sufficient condition for the space processing; to conduct careful analysis on each; and the re-examine the original premise as to its validity.

The premises which we examined are as follows:

1. "Space processing can be used to purify a low purity fused silica (SiO_2) glass preform in order to meet optical fiber standards."

    In order to test this premist, extensive calculations were made to convert known thermodynamic properties of various oxides into their vapor pressure (P_{vap}). The approach here was to compare the vapor pressure of each oxide with that of pure SiO_2, both as pure substance. From it, one can select the oxide component which might be eliminated from SiO_2 glass through evaporation. Detailed description of the calculations, as well as the results, are included in Appendix 1. The vapor pressures are plotted versus $1/T$ for various oxides including SiO_2, as shown in Figure 1. We calculated also the change in vapor pressure (Δp) due to the change of external pressure from 1 atm. on earth to about 10^{-11} torr in space. Results are included also in Appendix 1, as well as plotted in Figure 2. In Table 1, the (P_{vap}) and Δp values for various oxides at $2000^{\circ}K$ are listed for comparison.
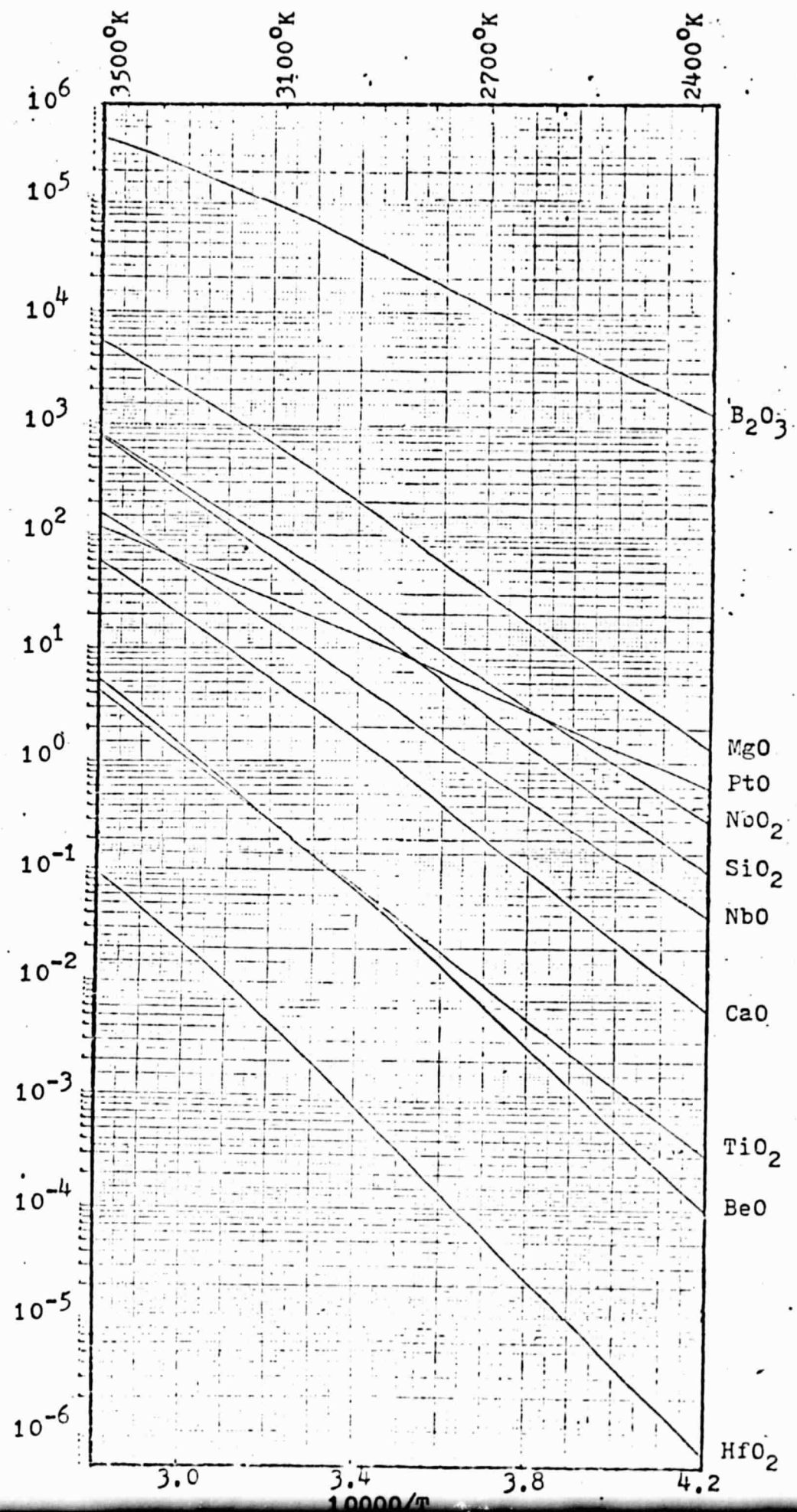
    It is shown that SiO_2 has fairly high vapor pressure as compared to many of the oxides studied here. Purification requires that the impurity oxides must have higher vapor pressures than that of SiO_2 at the purifying temperature. Among the oxides studied here, only B_2O_3 and MgO fulfill this first requirement. ——

    From the vapor pressure calculations, the impurity contents in equilibrium with the glass melt was calculated. The results are included in Table 1-2, Appendix 1. At $2500^{\circ}K$, the MgO content at equilibrium in SiO_2 glass was determined to be 5.4×10^4 ppm. The B_2O_3 content was 1.46×10^2 ppm. In both cases, the impurity contents increase with temperatures greater than $2500^{\circ}K$. This is due to the greater rate of evaporation for SiO_2 as compared to B_2O_3 and MgO. This calculation serves as a lower bound of the impurity content due to evaporative purification processes. It is clear, therefore, that space processing is not able to purify low purity SiO_2 glass preform to the high purity standards for the optical fiber application.

2. "Space processing can be used to modify the glass composition profile so as to satisfy the requirement of optical fiber."

Vapor Pressure Change, ΔP (Torr)

B_2O_3

MgO
PtO
NbO_2
SiO_2

NbO

CaO

TiO_2

BeO

HfO_2

$3500^\circ K$ $3100^\circ K$ $2700^\circ K$ $2400^\circ K$

10^2
10^1
10^0
10^{-1}
10^{-2}
10^{-3}
10^{-4}
10^{-5}
10^{-6}
10^{-7}
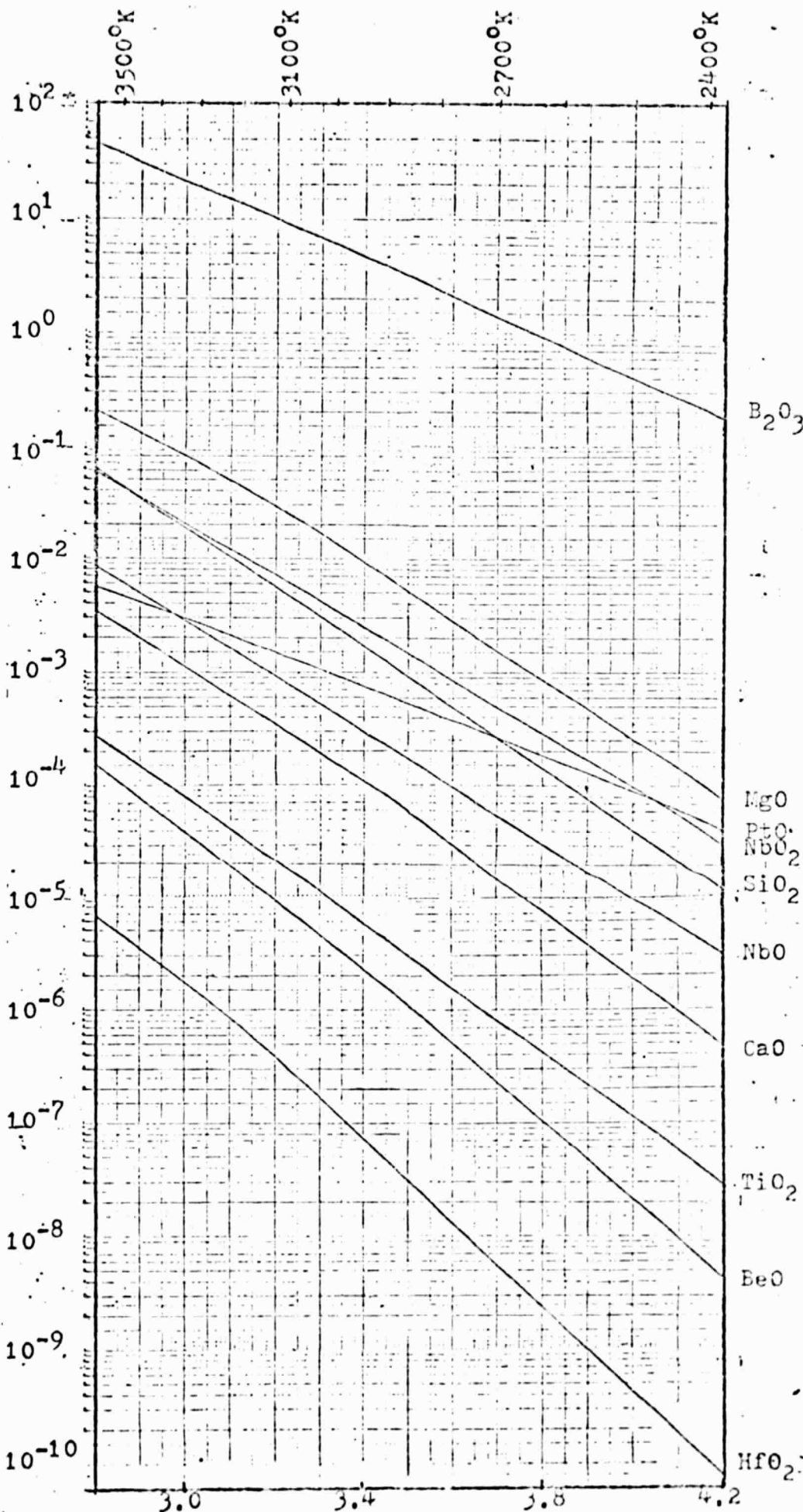10^{-8}
10^{-9}
10^{-10}

3.0 3.4 3.8 4.2

Table 1

Vapor pressures $(V_A)_p$ and changes in vapor pressures due to vacuum exposure $(\Delta (V_A)_p)$ of various constituent oxides at $2000^\circ K$.

	$(V_A)_p$ (torr)	$\Delta (V_A)_p$ (torr)
SiO_2	0.495×10^{-3}	0.682×10^{-7}
SiO	0.377×10^{10}	0.476×10^{6}
PtO	0.243×10^{-1}	0.210×10^{-5}
NbO_2	0.183×10^{-2}	0.236×10^{-6}
NbO	0.200×10^{-3}	0.182×10^{-7}
MnO	0.470×10^{4}	0.375
MgO	0.810×10^{-2}	0.556×10^{-6}
HfO_2	0.407×10^{-9}	0.539×10^{-13}
CaO	0.163×10^{-4}	0.165×10^{-8}
BeO	0.118×10^{-6}	0.597×10^{-11}
TiO_2	0.108×10^{-5}	0.635×10^{-9}
B_2O_3	0.360×12^{2}	0.622×10^{-2}

In order to increase the band width of the optical fiber transmission, it is necessary to decrease the dispersion. As indicated in Appendix 5, one of the very effective means to lower the dispersion it to have a graded refractive index profile in the fiber core. Currently, the graded index profile is achieved by either ion exchange processes or the concurrent doping during the CVD (flame pyrolysis) process.

We explore the possibility that viscous flow process can be set in a laminalar fashion so as to set up a sharper step function type of grading in refractive index. Fluid mechanical analysis[1,2] indicated that interface between two viscous liquids can be very complicated and no stable shapes of a rotating liquid exist. Our analysis confirms that the possibility of producing a concentric annular layer of two glass compositions by the viscous flow processes in the space processing conditions is very remote. Later, we found out through private communications from Dr. D. Gloge and Dr. D. Marcuse of Bell Telephone Lab - Crawford Hill that step function type of index gradient is not desirable from the lowering dispersion viewpoint.

Another feasibility is to achieve a gradual graded refractive index through evaporation. The vapor pressure calculations which we conducted convinced us that it is unreasonable to expect the evaporative process in SiO_2 can purify the impurity contents to the ppb ranges which are required. However, the evaporative mechanism, coupled with bulk diffusion process, can change the chemical composition continuously from the surface to the center of the bulk so as to generate a graded index profile. For that purpose, we were supplied with the computer program on evaporative kinetics by Dr. Robert Paule of NBS, which was developed in conjunction with his work for a NASA contract.[3] Dr. Paule's program calculates the kinetics of evaporation. It gives the amounts of gaseous molecules, probably generated in the process of evaporation, as a function of time and the initial impurity content. The gaseous molecules include all possible species, and the kinetics calculations involve all complex

equilibria, based on thermodynamic quantities. Brief description of his approach is given in Appendix 2. The conversion of his program, which was originally written for a CDC computer, to be used in an IBM 370/155 computer took longer time than expected. Only recently since our 6th monthly report, we are able to complete the use of his program. We tested the program with one of the test data which Dr. Paule kindly supplied us. Now, we have run a program which gives the results of B_2O_3 evaporation in a SiO_2 glass. The data are shown in Table 2. Drs. Paule's program gives the partial vapor pressures as a function of time and temperature. It also gives the moles as a function of time and temperature. From this set of results, it will enable us to construct the refractive index profile as modified by evaporation. This appears to be a clear benefit for the space processing of glass preform.

3. "Evaporative processes will generate bubbles in a glass medium. Space processing conditions will allow the removal of these bubbles from the glass preforms so as to maintain their optical qualities."

This point was recognized by us as one of the notable troublesome problems about the space processing of glass preforms. Evaporative processes will generate bubbles. Any rotation will tend to accumulate all the bubbles toward the central portion of the glass preform. Such a result will eliminate the use of the glass preform for optical fiber transmission applications.

We studied this problem extensively. We studied first the change of bubble radius when the bubble is stationary and it is subject to a sudden change of external pressure from 1 atm. to 10^{-11} torr. This relates to the bubbles already existing in the glass preform prior to the space processing and their response to the space environment. Detailed description of the solutions of this problem is included in Appendix 3. Representative data from the numerical solutions (Runge-Kutta method) are presented in Figures 3 and 4, and Table 3 and 4. Transient response curves at temperatures of 2250°, 2500°, 2750°, 3000°, 3250°, and $3500^\circ K$ are shown in Figure 5. This behavior can be generalized, as shown in Figure 6, for various values of A,

TABLE 2

COMPLEX EQUILIBRIUM REACTIONS INVOLVING

PRESSURES OF SPECIES PRESENT IN ATMOSPHERES

	TEMP(K) 2000.	2000.	2000.
	TIME(sec) 0.0005	0.100	1.000
SIO2	0.0	0.0	0.0
B2O3	0.0	0.0	0.0
TGAS	0.53475146010D-06	0.53115423720D-06	0.50469737560D-06
O2	0.28542220420D-07	0.28286453630D-07	0.26009802500D-07
B	0.78326101990D-14	0.70232112130D-14	0.77374469070D-14
B2	0.41055003360D-26	0.40950532000D-26	0.40063457680D-26
BO	0.39266871590D-06	0.39343643610D-06	0.37029022130D-06
BO2	0.34006030350D-21	0.33660880560D-21	0.30612348710D-21
B2O	0.26459799580D-15	0.26277607710D-15	0.24648679590D-15
B2O2	0.76707142800D-09	0.75857478160D-09	0.68213084520D-09
SI	0.55759181900D-11	0.56203533400D-11	0.61188175520D-11
SIO	0.64600377940D-09	0.64691771590D-09	0.67672300770D-09
O	0.11212188070D-06	0.11101642000D-06	0.10703237120D-06

MOLES OF SPECIES PRESENT

	TEMP(K) 2000.	2000.	2000.
	TIME(sec) 0.0005	0.100	1.000
SIO2	0.10000000000D 01	0.99999999960D 00	0.99999999570D 00
B2O3	0.99999202451D-05	0.98414449110D-05	0.84883124660D-05
TGAS	0.22880377990D-08	0.45200344360D-06	0.38901592080D-05
O2	0.10590215130D-09	0.20806590337D-07	0.17354682290D-06
B	0.45952307950D-16	0.55285779500D-14	0.88821755370D-13
B2	0.18513994880D-28	0.36154470050D-26	0.32520341610D-25
BO	0.15902000930D-08	0.31405074340D-06	0.26992327770D-05
BO2	0.10898833694D-23	0.21467501440D-21	0.17659303380D-20
B2O	0.90458126640D-18	0.17817549010D-15	0.15167965140D-14
B2O2	0.21965762360D-11	0.43216272040D-09	0.35160155430D-08
SI	0.22062434130D-13	0.44301195990D-11	0.43578989940D-10
SIO	0.20401715600D-11	0.40782533350D-09	0.38469380810D-08
O	0.58777669340D-09	0.11044230860D-06	0.10099729860D-05

Transient Response of Bubbles, Temp (C): 2500.0 Pressure in Vacuum (Dyne/Cm/Cm): 0.1000-15 Original Bubble Radius (Cm):0.10 Specific Gravity, Surface Tension (Dyne/Cm), and Viscosity of Glass (Poise): 2.260 100.00 500.00 Initial Velocity of Bubble (Cm/Sec): 0.0 Horizontal Axis Represents Time in Seconds in Log Scale, Vertical Axis Represents Bubble Size Ratio to Its Original in Log Scale
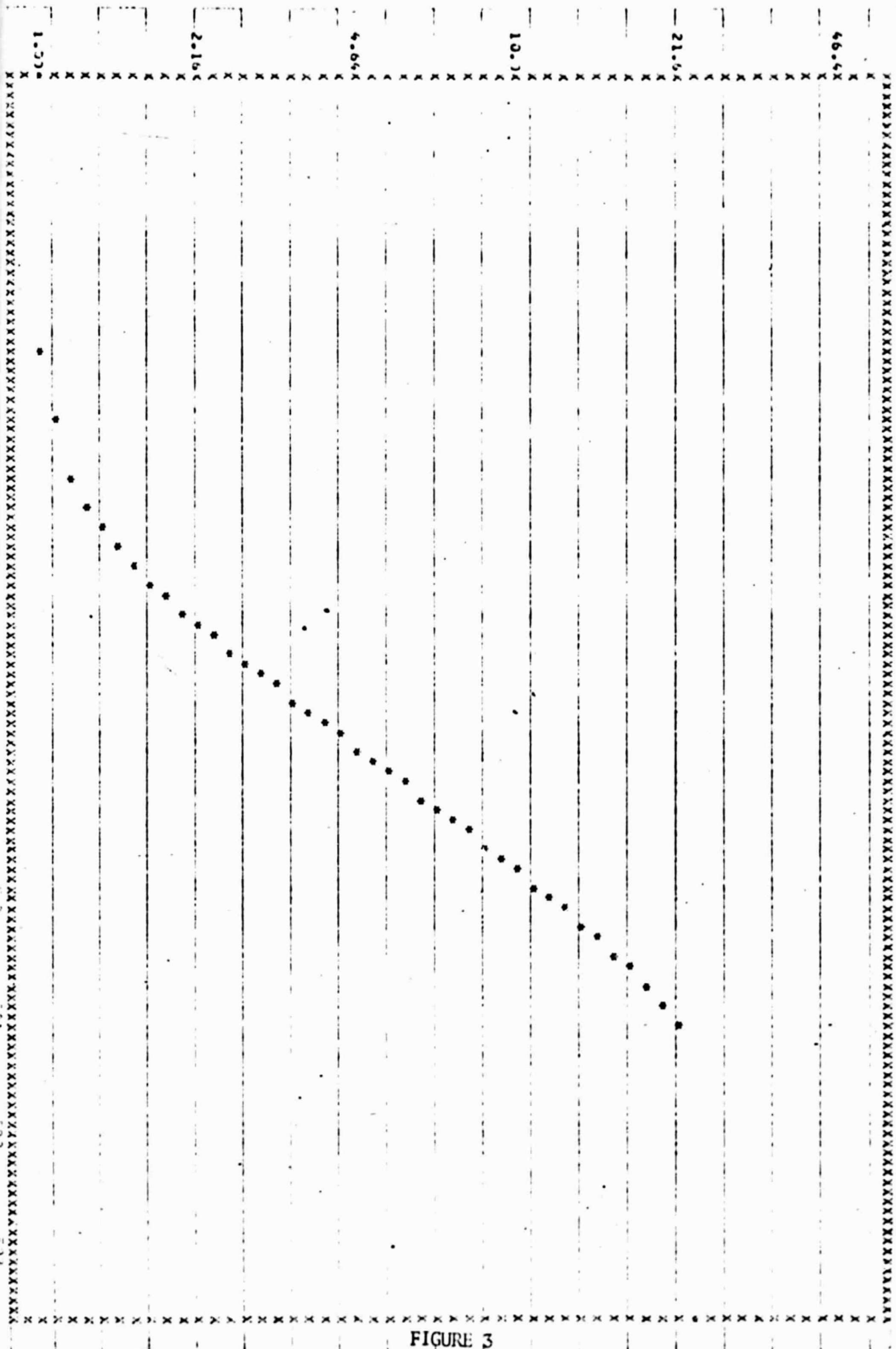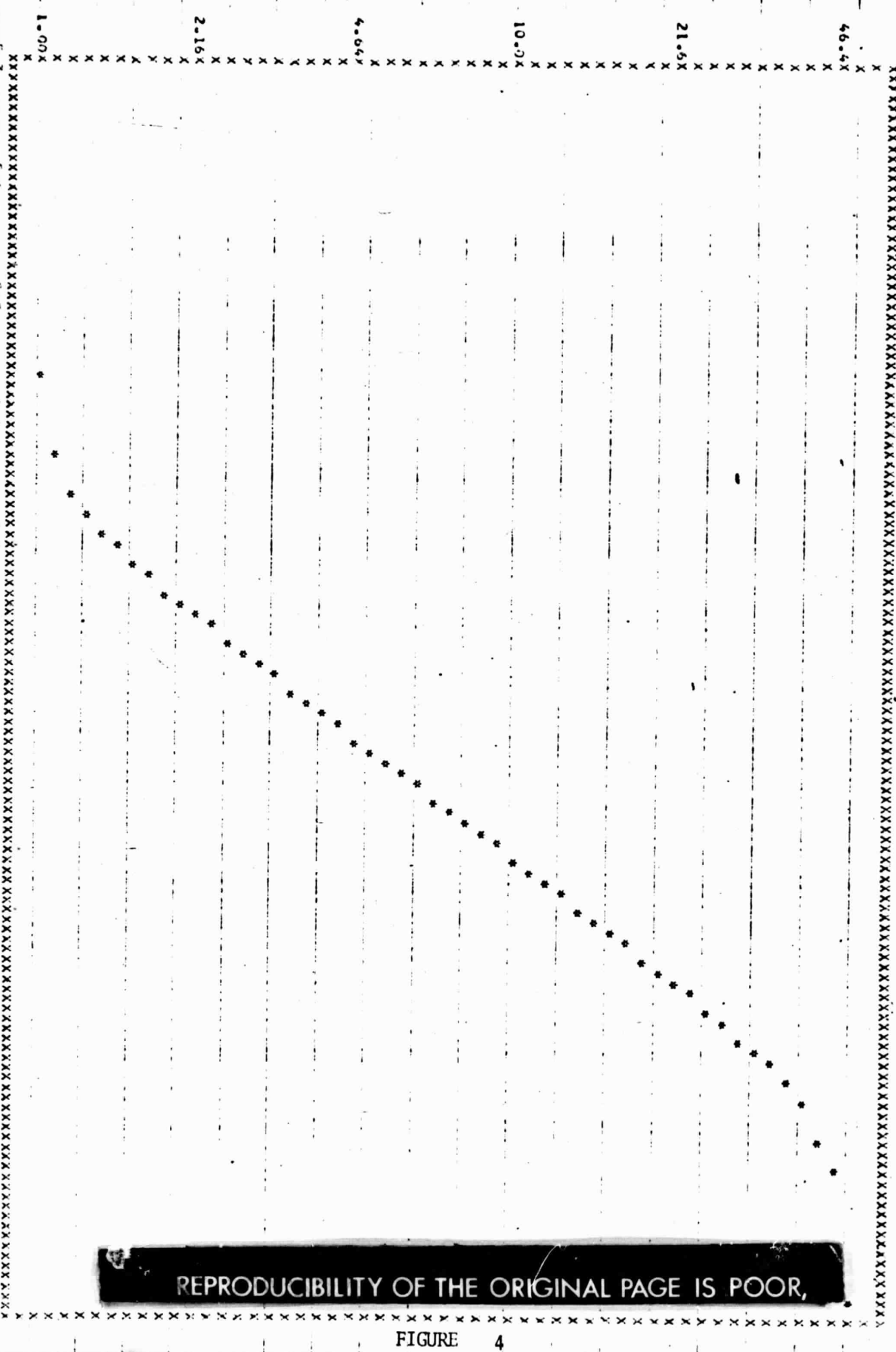

FIGURE 3

TABLE 3

Transient Response of Bubbles, Temp (C):2500.0 Pressure in Vacuum (Dyne/Cm/Cm): 0.100D-15 Original Bubble Radius (cm);0.10 Specific Gravity, Surface Tension (Dyne/Cm), and Viscosity of Glass (Poise):2.200 100.00 500.00 Initial Velocity of Bubble (Cm/Sec): 0.0 Columns I, II, III, IV represent Time Seconds, Radius of the Bubble, Size Ratio of the Bubble to Its Original and Pressure in the Bubble at That Time Respectively

TIME(SEC)	R(CM)	R/RO	P(DYNE/CM/CM)	% COMPLETE IN SIZE INCREASE
0.0	0.1000000 00	0.1000000 01	0.1035000 07	0.0
0.5000000-04	0.1063130 00	0.1063130 01	0.8613520 06	0.2902740 00
0.0	0.1000000 00	0.1000000 01	0.1035000 07	0.0
0.5000000-04	0.1020560 00	0.1020560 01	0.9737080 06	0.9452020-01
0.7500000-04	0.1032180 00	0.1032180 01	0.9411870 06	0.1470560 00
0.1000000-03	0.1043920 00	0.1043920 01	0.9097760 06	0.2019270 00
0.2000000-03	0.1089260 00	0.1089260 01	0.8208330 06	0.4164310 00
0.3000000-03	0.1131250 00	0.1131250 01	0.7149310 06	0.6054690 00
0.5000000-03	0.1206940 00	0.1206940 01	0.5886340 06	0.9515150 00
0.7500000-03	0.1289870 00	0.1289870 01	0.4822840 06	0.1332820 01
0.1000000-02	0.1363280 00	0.1363280 01	0.4084920 06	0.1670370 01
0.2000000-02	0.1598260 00	0.1598260 01	0.2535100 06	0.2750810 01
0.3000000-02	0.1778900 00	0.1778900 01	0.1838550 06	0.3561330 01
0.5000000-02	0.2058040 00	0.2058040 01	0.1137360 06	0.4486050 01
0.7500000-02	0.2324940 00	0.2324940 01	0.8235760 05	0.6092080 01
0.1000000-01	0.2541110 00	0.2541110 01	0.6307550 05	0.7056030 01
0.2000000-01	0.3164880 00	0.3164860 01	0.3254870 05	0.9954110 01
0.3000000-01	0.3606100 00	0.3606100 01	0.2207120 05	0.1198280 02
0.5000000-01	0.4254880 00	0.4254880 01	0.1343530 05	0.1496590 02
0.7500000-01	0.4853100 00	0.4853100 01	0.9054900 04	0.1771650 02
0.1000000 00	0.5327290 00	0.5327300 01	0.6665740 04	0.1989690 02
0.2000000 00	0.6660770 00	0.6660770 01	0.3592410 04	0.2602820 02
0.3000000 00	0.7579950 00	0.7579950 01	0.2376520 04	0.3025450 02
0.5000000 00	0.8399770 00	0.8399780 01	0.1468260 04	0.3632310 02
0.7500000 00	0.1008300 01	0.1008300 02	0.1009640 04	0.4176370 02
0.1000000 01	0.1074470 01	0.1074470 02	0.8343580 03	0.4480630 02
0.1000000 01	0.1099650 01	0.1099660 02	0.7783420 03	0.4596410 02
0.1999370 01	0.1343420 01	0.1343420 02	0.4266770 03	0.5717250 02
0.5002500 01	0.1720940 01	0.1720940 02	0.2193150 03	0.7361120 02
0.7496690 01	0.1857330 01	0.1857330 02	0.1615390 03	0.8080170 02
0.7502550 01	0.1857720 01	0.1857720 02	0.1614370 03	0.8081970 02
0.9994650 01	0.1961330 01	0.1961330 02	0.1371140 03	0.8559400 02
0.1000250 02	0.1951600 01	0.1951600 02	0.1371220 03	0.8559640 02
0.1998690 02	0.2160440 01	0.2160450 02	0.1026390 03	0.9473910 02
0.1999470 02	0.2160530 01	0.2160530 02	0.1026260 03	0.9474300 02
0.2000250 02	0.2160610 01	0.2160620 02	0.1026140 03	0.9474690 02
0.2001130 02	0.2161700 01	0.2161700 02	0.1026020 03	0.9475080 02
0.2997710 02	0.2229450 01	0.2229450 02	0.9339950 02	0.9791220 02
0.2998690 02	0.2229490 01	0.2229490 02	0.9339550 02	0.9791360 02
0.2999470 02	0.2229520 01	0.2229520 02	0.9339140 02	0.9791510 02
0.3000250 02	0.2229550 01	0.2229550 02	0.9338740 02	0.9791660 02
0.3001030 02	0.2229580 01	0.2229580 02	0.9338340 02	0.9791810 02
0.3001810 02	0.2229610 01	0.2229610 02	0.9337930 02	0.9791950 02
INFINITE	0.2274860 01	0.2274860 02	0.1218440 11	0.1000000 03

ORIGINAL PAGE IS
OF POOR QUALITY

TABL

Transient Response of Bubbles, Temp (C): 2500.0 Pressure in Vacuum (Dyne/Cm/Cm): 0.1000-15 Original Bubble Radius (Cm):0.50
Specific Gravity, Surface Tension (Dyne/Cm), and Viscosity of Glass (Poise): 2.260 100.00 500.00 Initial Velocity of
Bubble (Cm/Sec): 0.0 Horizontal Axis Represents Time in Seconds in Log Scale, Vertical Axis Represents Bubble Size Ratio to
Its Original in Log Scale

FIGURE 4

TABLE 4

Transient Response of Bubbles, Temp (C): 2500.0 Pressure in Vacuum (Dyne/Cm/Cm): 0.100D-15 Original Bubble Radius (Cm):0.50
Specific Gravity, Surface Tension (Dyne/Cm), and Viscosity of Glass (Poise): 2.260 100.00 500.00 Initial Velocity of Bubble:
(Cm/Sec): 0.0 Columns I, II, III, IV Represent Time in Seconds, Radius of the Bubble, Size Ratio of the Bubble to Its Original
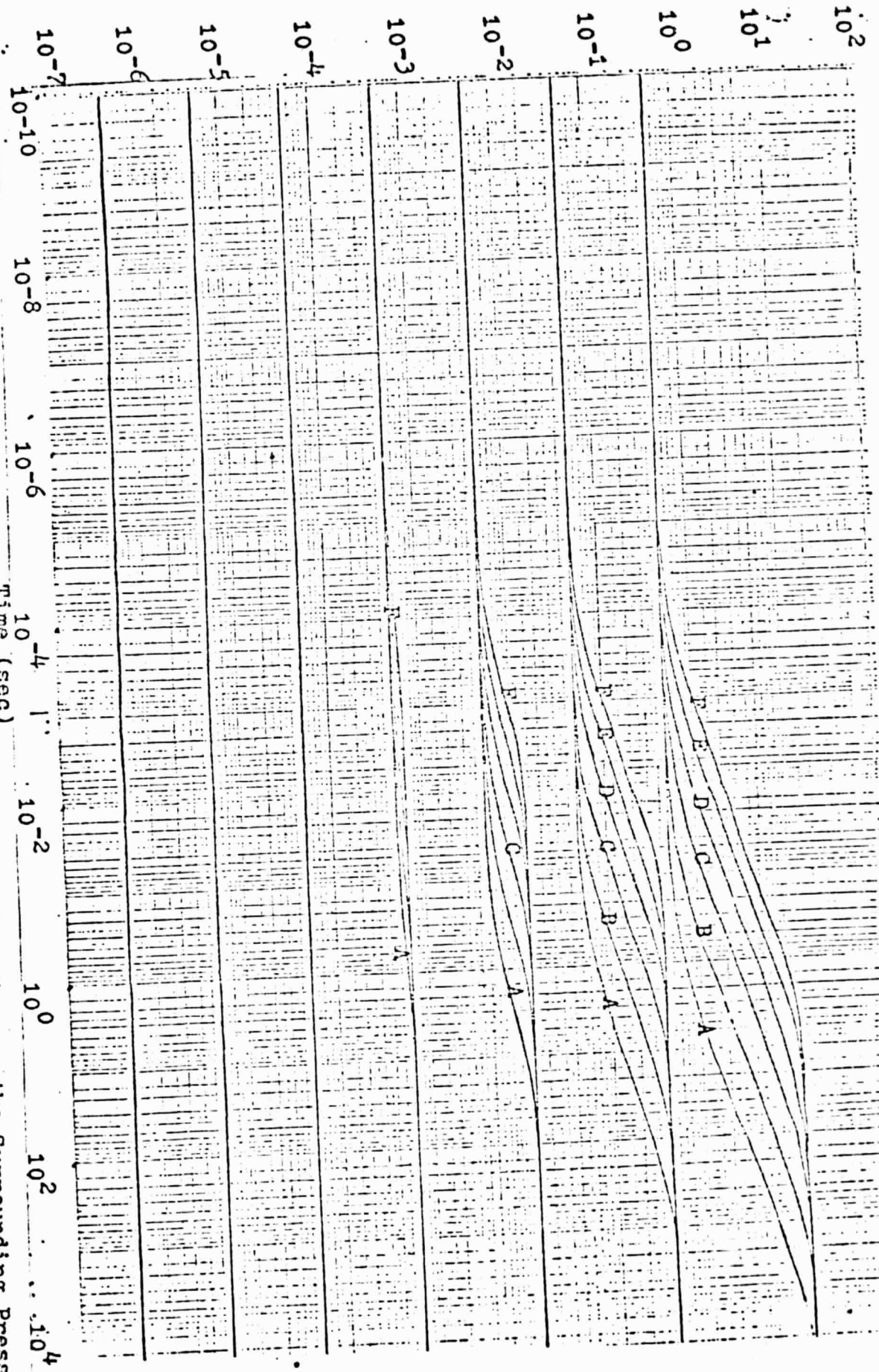Pressure in the Bubble at That Time Respectively

TIME(SEC)	R(CM)	R/RO	PB(DYNE/CM/CM)	% COMPLETE IN SIZE INCREASE
0.0	0.5000000 00	0.1000000 01	0.1033440 07	0.1270040 20
0.5000000-04	0.5010760 00	0.1002150 01	0.1026720 07	0.4317010-02
0.1000000-03	0.5040590 00	0.1008090 01	0.1004700 07	0.1621110-01
0.2000000-03	0.5147630 00	0.1029370 01	0.9502220 06	0.5092810-01
0.3000000-03	0.5279990 00	0.1055600 01	0.8775430 06	0.1125840 00
0.5000000-03	0.5605260 00	0.1121050 01	0.7336650 05	0.2429390 00
0.7500000-03	0.6027350 00	0.1205430 01	0.5899270 06	0.4125990 00
0.1000000-02	0.6427520 00	0.1285560 01	0.4864670 06	0.5729770 00
0.2000000-02	0.7743590 00	0.1548080 01	0.2785410 06	0.1099940 01
0.3000000-02	0.8733150 00	0.1746660 01	0.1949390 06	0.1426410 01
0.5000000-02	0.1022600 01	0.2045760 01	0.1207060 06	0.2093120 01
0.7500000-02	0.1162900 01	0.2325750 01	0.8216040 05	0.2660730 01
0.1000000-01	0.1275000 01	0.2549990 01	0.6232250 05	0.3110680 01
0.2000000-01	0.1599250 01	0.3198500 01	0.3182060 05	0.4396030 01
0.3000000-01	0.1820560 01	0.3641130 01	0.2140720 05	0.5304670 01
0.5000000-01	0.2151500 01	0.4303600 01	0.1296509 05	0.6629790 01
0.7500000-01	0.2479090 01	0.4958390 01	0.8698310 04	0.7829900 01
0.1000000 00	0.2744000 01	0.5403260 01	0.6550890 04	0.8550200 01
0.2000000 00	0.3392950 01	0.6785900 01	0.3307090 04	0.1101170 02
0.3000000 00	0.3876370 01	0.7752740 01	0.2217100 04	0.1355210 02
0.5000000 00	0.4583200 01	0.9166520 01	0.1341700 04	0.1658940 02
0.7500000 00	0.5232900 01	0.1046580 02	0.9014700 03	0.1892650 02
0.1000000 01	0.5747060 01	0.1149420 02	0.6804590 03	0.2106090 02
0.2000000 01	0.7149950 01	0.1430390 02	0.3472470 03	0.2466020 02
0.3000000 01	0.8189050 01	0.1637810 02	0.2355060 03	0.3005840 02
0.5000000 01	0.9620020 01	0.1924000 02	0.1450940 03	0.3660590 02
0.7500000 01	0.1090540 02	0.2181250 02	0.9957490 02	0.4176060 02
0.1000000 02	0.1201450 02	0.2360250 02	0.7662070 02	0.4516300 02
0.2000000 02	0.1457060 02	0.2914120 02	0.4175870 02	0.4917060 02
0.3000000 02	0.1628370 02	0.3256710 02	0.2991720 02	0.6335250 02
0.5000000 02	0.1853120 02	0.3706240 02	0.2029800 02	0.7231350 02
0.7500000 02	0.2030340 02	0.4060600 02	0.1543300 02	0.7743660 02
0.1000000 03	0.2149900 02	0.4299300 02	0.1300340 02	0.8421080 02
0.2000000 03	0.2367000 02	0.4733200 02	0.9502310 01	0.9313710 02
0.3000000 03	0.2474790 02	0.4949580 02	0.8572430 01	0.9752020 02
0.5000000 03	0.2528150 02	0.5056300 02	0.7994110 01	0.9967700 02
0.7500000 03	0.2539590 02	0.5079170 02	0.7884550 01	0.9926920 02
0.9995000 03	0.2539990 02	0.5082310 02	0.7872000 01	0.9998590 02
0.1000000 04	0.2541150 02	0.5082310 02	0.7871990 01	0.9993490 02
0.2000000 04	0.2541410 02	0.5082810 02	0.7869660 01	0.1000000 03
0.3000000 04	0.2541410 02	0.5082910 02	0.7869660 01	0.1000000 03
INFINITE	0.2541410 02	0.5082810 02	0.1357000 12	0.1000000 03

Table 3

radius of bubbles(cm)

Time (sec)

Transient Response of Bubbles Imbedded in Silicon Dioxide Medium as the Surrounding Pressure
suddenly changes from 1 atm to Vacuum. Curve A(T=2250°K), B(2500°K), C(2750°K), D(3000°K),
E(3250°K), and F(3500°K).

FIGURE 5

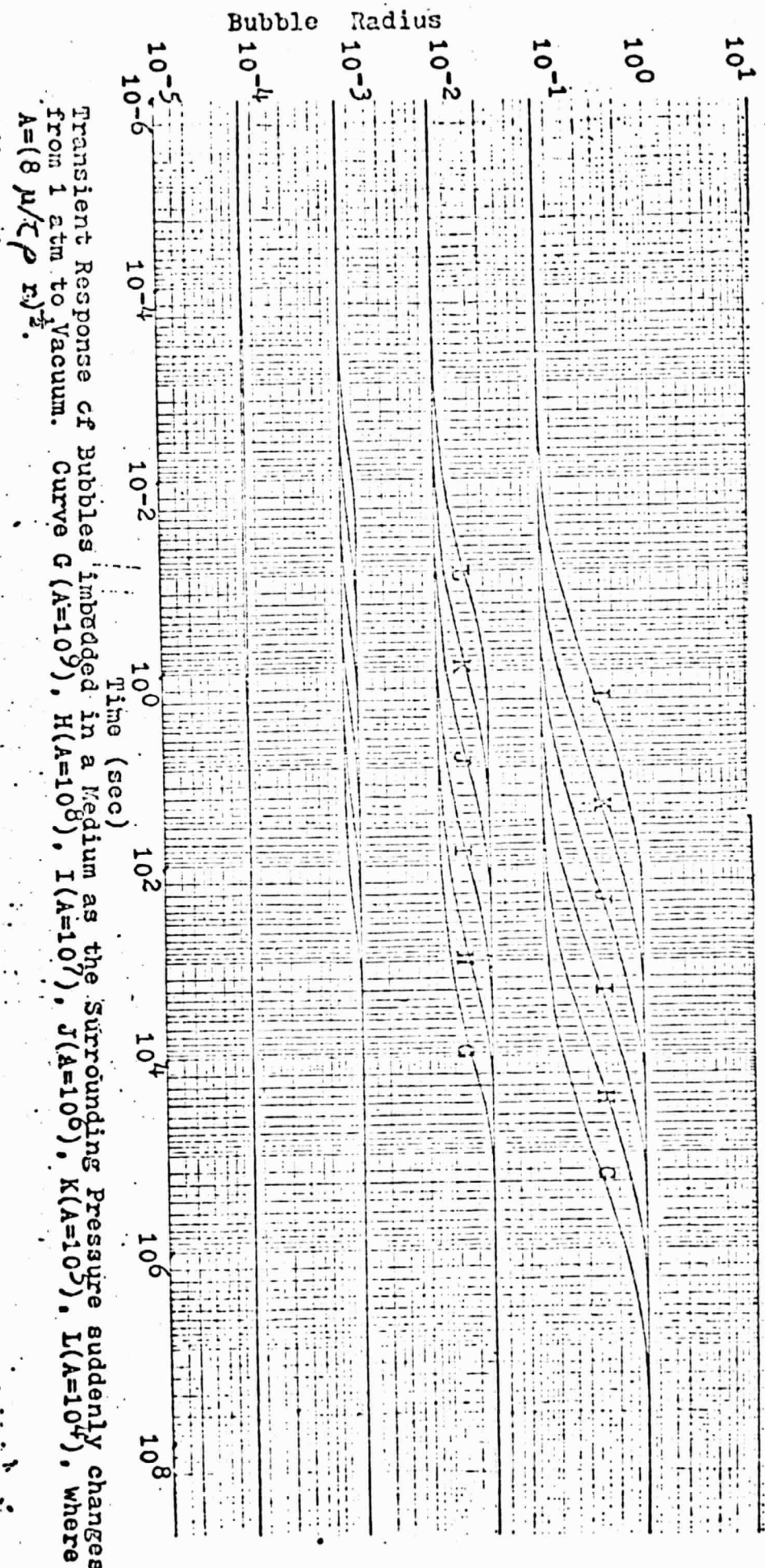Bubble Radius

Time (sec)

Transient Response of Bubbles imbedded in a Medium as the Surrounding Pressure suddenly changes from 1 atm to Vacuum. Curve G $(A=10^9)$, H$(A=10^8)$, I$(A=10^7)$, J$(A=10^6)$, K$(A=10^5)$, L$(A=10^4)$, where $A=(8\mu/K\rho\, r_i)^{\frac{1}{2}}$.

FIGURE 6

where $A = (8\mu/\tau\rho r_0)^{\frac{1}{2}}$.

At large R values, equation (3-1) can be simplified to equation (3-2) by neglecting the inertia force term. Equation (3-2) can be analytically solved. As shown in Table 5, this analytical solution of equation (3-2) produces errors of less than 1% when R is greater than 0.1 cm.

The results showed that after 1 second of time duration, the bubble grows to 44.8% of its ultimate size, for the case of original bubble size of 0.10 cm. as shown in Table 3. This change in bubble size means that there will be internal convective forces inside the glass medium. It will be to our advantage if such convective forces can be utilized to fine bubbles from the glass medium.

We analyzed also the case of the bubble with an initial velocity. It is clear that bubbles can be manipulated under the space processing conditions. We have been in contact with Dr. Taylor Wang of JPL who has constructed an acoustic chamber for weightless positioning.[4] His acoustic chamber can be utilized to accomplish our purpose - to remove the bubbles from the glass preform during the space processing. Conceptually, it is feasible. But the basic premises must be experimentally confirmed by simulated tests. This ability to remove bubbles is a must condition in order for any space processing to succeed. Both theoretical and experimental efforts are required to solve this problem.

4. "Space processing should be able to offer a clear advantage to the processing of glass preform."

One of the great advantages of the space processing is the zero-gravity condition. This enables the processing to disregard sizes and weight. In the current practices, the glass preform consists of a central glass rod, sealed to a glass tubular envelope, with the interior between them be evacuated to vacuum. During the sealing process on earth, both the glass rod and the glass envelope are placed on a lathe. Both are heated and both are being rotated. Good sealing requires the glass to be relatively fluid. Rotation of this molten glass will cause local distortion due to sagging. This condition places a limit to the size of glass preform which

Table 5

Comparison between the results by the numerical method, and by the analytical approximation (neglecting the inertia force term).

Temperature = $3500^\circ K$

r_o = initial bubble radius = 0.05 cm

t = time in seconds required to reach $r = R$

R = bubble radius in cm. at the time t.

R.E. = relative error of the analytical approximation

$$\equiv \frac{|\, t_{num.\ method} - t_{anal.\ approx.} \,|}{t_{num.\ method}}$$

	R (cm)	t (sec.) num. method	anal. approx.	R.E. %
1.	0.50617×10^{-1}	0.2×10^{-5}	0.141647×10^{-6}	92.91
2.	0.55575×10^{-1}	0.65×10^{-4}	0.518925×10^{-4}	20.16
3.	0.84649×10^{-1}	0.55×10^{-3}	0.542993×10^{-3}	1.274
4.	0.10418	0.1150×10^{-2}	0.114898×10^{-2}	0.088
5.	0.29841	0.438×10^{-1}	0.441039×10^{-1}	0.069
6.	0.41045	0.5638×10^{-1}	0.568079	0.074

can be formed on earth, as shown in Appendix 4. In space, the limitation is less
is less severe. As shown in Table 6, space processing will allow the production of
glass preform with greater radius. This difference has a significant impact on the
cost per km length of glass fiber optics which eventually is produced from the glass
preform. The size relationship between the glass preform and the glass fiber optics
is shown in Table 7. The first row figures represent the sizes used in the current
practice. As shown in Table 8, this difference can mean a cost of 8.471 ¢/km for glass
fiber prepared on earth, and a cost as low as 1.964¢/m   for glass preforms processed
in space. This set of cost figures reflects the material cost. The current market
price for a 19 fiber bundle (Corning Glass Works, quoted in Electronics, June 13, 1974)
is $57 per meter for an order of less than 5 km. The maximum length available is
500 m.

Since the market price is so high, and the availability is not general, it
is certain that the space processing of glass preform offers to any manufacturer the
opportunity to make their own fiber economically without the extensive and expensive
capital investment in the preparation of glass rod and glass envelope. In other
words, any manufacturer can afford to pay the high price for the high purity glass
rod and glass envelope from vendors, and to space process the glass preform in larger
diameter sizes, and then to draw the optical fiber from the glass preform in a simple
earth-bound operation. This way, the manufacturer can have the fiber exactly to his
own requirement, with equal or better properties, and with cheaper total cost than
relying on the major supplier for the fiber. From this viewpoint, it is certain that
space processing of glass preforms will have commercial customers.

Space processing can offer other advantages in the glass preforms it produces.
As stated in Appendix 5, in order to lower the dispersion it is best to employ means
to facilitate mode coupling. Graded index profile is one of the mode coupling mech-
anisms. Space processing is possible to contribute to this, as stated before. In
addition, a fiber with geometrical variations along the longitudinal direction can

TABLE 6

Limiting maximum glass tubing radii

Earth bound location, $\Delta P_1 = 10^{-4}$ atm $= 101.3$ dyne/cm^2,

w (rad/sec)	r (cm)
10	0.559
1	0.560
0.1	0.561

Space shuttle laboratory

w (rad/sec)	r (cm)
10	1.18
1	5.51
0.1	25.6

TABLE 7

Size relationship between glass preform and

glass fiber optics

Diameter of preform		Length (L_p) of preform		O.D. of glass fiber optics	Length (L_g) of fiber drawn from the preform	$\dfrac{L_g}{L_p}$
inch	cm	inch	m	μm	km	km/m
0.250	0.635	30	· 0.762	85	4.25	5.577
2.250	5.715	1.0	0.0254	85	10.67	420.079
5.0	12.7	1.0	0.0254	85	230.40	9070.866

TABLE 8

Cost per km length of glass fiber optics

Diameter of preform	Length of preform	Cost of Materials	Cost of transport to space	Length of glass fiber optics drawn	Cost per m of glass fiber optics	Processing location
inch	inch	$	$	km	¢/ m	
0.250	30	360.	———	4.25	8.471	earth
2.250	1.0	739.	47.	10.67	7.366	space
5.0	1.0	3,510.	1,015.	230.40	1.964	space

also have effective mode coupling. Of course, dimensional precision of glass pre-forms is a prerequisite for it insures the diameter stability of the optical fiber. Usually, it is required to have a variance in diameter of less than 1 μm over a length of 200 m. of 50 μm diameter fiber. Supposing onto this diameter uniformity, a periodical diameter variance in a smooth functional fashion is desirable to promote mode coupling. Mode coupling reduces multimode delay spread in a factor of $\sqrt{\frac{L}{\ell_c}}$

where L is the fiber length, and ℓ_c is the coupling length.

We have investigated the possibility of making glass preform with sinusoidal surface modulation in the longitudinal direction. Previous works in the literature[5,6,7,8,9] demonstrated the relationships between the glass fiber diameter with the shaping diameter under molten glass conditions. In some cases,[6,7,8] dies were used for shaping. We shall substitute a shaping heating coil for the dies. By the use of levitation technique,[10] a shaping heating coil can be equally effective. In order to obtain a relationship in our scheme, a detailed fluid mechanical study must be undertaken.

Perhaps, the most important advantage which the space processing of glass preform can offer lies in the radiation resistance of the optical fiber. Recent studies[11,12,13] showed that doped silica glass is more sensitive to radiation than pure SiO_2 glass. Doped silica glasses, such as fused SiO_2 doped with GeO_2 or TiO_2 or B_2O_3, have slightly higher refractive index than SiO_2, and are used as the fiber core glass. Present radiation studies are preliminary and exploratory, and the level of radiation dosage is considerably higher in these studies than the possible levels used in optical fiber transmission. But the life expectancy of the optical fiber is very long and the fidelity of the fiber is required to be high. We have not investigated this aspect during this project. But we venture to state that space processing can produce, or cause, a doped silica glass to have less defects, and consequently, more radiation resistance. This premise, if proved to be correct,

would make the space processing of glass preforms the only possible process.

5. Power requirement:

For a temperature of 1704°C (3100°F), power required is 3.63 kw (22 V, 165 amps), and the heat loss is 4 kw. The total power required is, therefore, 7.63 kw. However, this figure is for a furnace with SiC heating elements. The total weight is too high to be suitable for space processing operations. Consequently, a special furnace must be designed. For this study, the heating zone need not be greater than 1", and the heating chamber should be able to contain 10" diameter samples. The top temperature is preferred to be.about 2500°C, but a temperature of 1700°C is suffic-ient to do the job.

III. CONCLUSION

1. Space processing is unable to evaporatively purify the glass preform to the ppb range of impurity contents which optical fiber transmission applications requires.

2. Space processing should be able to modify glass composition and therefore to produce graded refractive index profile in the glass preform. This means lowers the dispersion of the optical fiber.

3. Space processing enables the production of larger diameter glass preform and thereby lowers the cost from a price of 8.471 ¢/m for earth bound operation to 1.964 ¢/m for space processing.

4. Space processing offers manufacturing opportunity to all customers in producing optical fibers of their own requirement at a cost cheaper than relying on sup-pliers.

5. Space processing can produce diameter modulation in the glass preform which promotes mode coupling and lowers the dispersion.

6. Space processing may produce, or cause, a doped silica glass preform to have less defects and consequently, more radiation resistent.

7. Power requirement: 7.63 kw

   Heating Zone 1"

   Heating chamber able to contain 10" diameter samples.

   Special furnace design is required

IV. POSSIBLE PLANS OF FUTURE

1. Study should be conducted on the evaporative purification kinetics, using the Paule's program, and their effects on graded refractive index profile.

2. Study should be conducted, in conjunction with Dr. Taylor Wang of JPL, on the removal of bubbles, or perhaps, defects from the glass preforms.

3. Study should be conducted on the design of heating coil and furnace in order to produce diameter modulation in the glass preform.

4. Study should be conducted on the effect of space processing on the radiation resistent properties of glass preforms.

V. PERSONNEL

Personnel working on this project include:

Professor Franklin F. Y. Wang

Professor Patrick J. Herley

Dr. Chandra Khattak

Mr. C. H. Lin	Graduate Student
Mr. H. C. Lin	Graduate Student
Mr. Gary Hanington	Graduate Student
Mr. Robert Lukachinski	Graduate Student
Mr. Donald Seidenspinner	Undergraduate Student
Miss Mary Faith Hughes	Undergraduate Student
Miss Perina C. M. Wu	Undergraduate Student

Data:

(1) K_p as a function of T are available in table form for various oxides. (Reference: "Thermodynamics of Certain Refractory Compounds" by Harold L. Schick, Academic Press, New York, vols. I and II (1966).[14]

(2) Data of K_p are given in $100°K$ increments.

Equations:

(1) Vapor pressure:

$$(p_{vap})_{pure\ substance} = \frac{(K_p)_v}{(K_p)_c} \times 760 \ (torr)$$

$(1-1)$

(2) Change in vapor pressure due to the change of external pressure from 1 atm. to 10^{-11} torr.

$$\Delta p = P \frac{V_c \cdot \Delta P}{RT}$$

$(1-2)$

Results:

(1) Results of P_{vap} (under column heading VAP PR) and ΔP (DEL VAP PR) are shown in the following tables (Table 1-1).

(2) Results include those for oxides such as: SiO_2; B_2O_3; MgO; PtO; NbO_2; NbO; CaO; TiO_2; BeO; and HfO_2.

(3) Interpolations of the vapor pressure results were made by the least square method.

First order approximation uses

$$P_{vap} = a \exp (b/T)$$

$(1-3)$

Second order approximation uses

$$P_{vap} = a \exp (b/T + c/T^2)$$

$(1-4)$

(4) Error for the first order approximation is 1.556%, and error for the second order approximation is 0.13%.

(5) Results of partial vapor pressures and parts per million of impurity oxides in SiO_2 are included in Table 1-2.

Explanations:

(1) Eq. (1-1) converts the results of equilibrium constants K_p to the vapor pressure of a pure substance. This is a straight-forward calculation.

(2) Eq. (1-2) converts the vapor pressure data at the earth condition of 1 atm. to those of the outer space condition (assumed to be 10^{-11} torr).

(3) In Table 1-1, vapor pressure results were calculated for substances whose equilibrium constants were already tabulated. Interpolations of the results used eqs. (1-3) and (1-4). All these results are for single pure substances.

(4) Using the results from Table 1-1, results were calculated and shown in Table 1-2 which gave the amount of oxide in ppm. which will be at equilibrium with pure SiO_2.

Appendix 2

Computer Program by Dr. Robert Paule of NBS
on the Calculation of Complex Equilibria Involving Vaporization
into Vacuum

Dr. Robert Paule of Inorganic Chemistry Section, National Bureau of
Standards, Washington, D. C. has developed calculations for describing
evaporative purification of materials in vacuum. The calculations have
been incorporated into a large Fortran computer program usable in a CDC
time sharing computer of 6000 series. Dr. Paule's work is sponsored by a
NASA contract W-13, 475 #3. Detailed description of his approach can be
found in his NASA reports. Briefly, his approach can be stated as follows:

"This basic program is to determine the number of moles of all species
present in a system, and to determine the distribution of these moles
between the various physical phases. For our general analytical approach
we want to work with the minimum information needed to fully determine the
physical and chemical system. This is equivalent to specifying a set of
independent physical properties and independent chemical species. In sim-
plest terms, our task is to solve one mass balance equation for each inde-
pendent chemical species. In this process we shall require that the equi-
librium constant relationships between the independent and dependent chemical
species be maintained. This problem could also be cast in terms of the
free energy".

A brief explanation of the computer printout results, obtained through
the Paule's program, in Table 2 is as follows:

1. The results are presented in two sections. The first section gives the results of partial vapor pressures of various species in units of atmosphere. The second section gives the results of moles of these species.

2. The major feature of Dr. Paule's program is to consider all possible gaseous species present in the reaction and their vaporation rates as a function of time and temperature.

3. In Table 2, the possible species include O_2, B, B_2, BO, BO_2, B_2O, B_2O_2, Si, SiO, O and total gases.

4. Initial concentration of SiO_2 (solid) was fixed to be at 1.0 mole, and 1×10^{-5} mole for B_2O_3 (solid).

5. Results in Table 2 were given at the temperature of $2000^{\circ}K$, and at three time intervals, namely 0.0005, 0.1, and 1 second.

6. Results in Table 2 indicate completely the kinetics of vaporation for an intial sample of 1 mole SiO_2 containing 1×10^{-5} mole B_2O_3.

APPENDIX 3   TRANSIENT RESPONSE OF A BUBBLE IMBEDDED IN

                                        MOLTEN GLASS SUBJECT TO A STEP DROP OF PRESSURE

                                        IN THE SURROUNDING.

For a spherical symmetrical bubble, which is stationary the equation for
the change of bubble radius is,

$$\ddot{R} + 3\dot{R}^2/2R + 4\mu\dot{R}/\rho R^2 + 2\tau/\rho R^2 = \left[(P_\infty + 2\tau/R_0)\ (R_0/R)^3 - P_\infty\right]/\rho R.$$

$$(3\text{-}1)$$

Numerical solution of eq. (3-1) was by the Runge-Kutta method. Computations
were done on IBM 370/155.

Analytical approximation which neglects the inertia terms in eq. (3-1), i.e.,
$\ddot{R} + 1.5\ \dot{R}^2/r$, gives

$$4\mu R/\rho R^2 + 2\tau/\rho R^2 = \left[(P_\infty + 2\tau/R_0)\ (R_0/R)^3 - P_\infty\right]/\ R$$

      viscous   surface
    force term   tension term

$$(3\text{-}2)$$

At large R values, the analytical approximation (eq. 3-2) produces errors
of less than 1% when R is greater than 0.1 cm, as compared to numerical
solution of eq. (3-1) as shown in Table 3-1.

Equations for the radius change of spherical bubble with an initial velocity
are:

$$R\ddot{R} + 2\dot{R}^2 + 4\mu R/\rho R + 2t/\rho R = P_\infty (R_0/R)^3/\rho$$

$$(3\text{-}3)$$

$$R\dot{v} + 3R\dot{v} + 6\nu v/R = o$$

$$(3\text{-}4)$$

where ρ is the density of molten glass

τ is the surface tension of molten glass

μ is the viscosity of molten glass

P_∞ is the pressure of surroundings before the step pressure change

P'_∞ is the pressure of surroundings after the step pressure change

R_o is the initial radius of gas bubble

R is the radius of gas bubble

Conducting the sealing operation in a earth bound location, the limiting
size (the maximum tube radius) of the glass tubing is given by the equation:

$$\rho \omega^2 w r^3 - (\rho g w \cos\sigma + \Delta P_1) r^2 - \tau w = o$$

$$(4\text{-}1)$$

In space shuttle laboratory, where

$$g = o$$
$$\Delta P_1 = o$$

$$(4\text{-}2)$$

the limiting size is given by:

$$r = (\tau / \rho \omega^2)^{1/3}$$

$$(4\text{-}3)$$

where ρ is the density of molten glass

ω is the angular velocity of the glass tubing

τ is the surface tension of molten glass

W is the wall thickness of the glass tubing

σ is the angular position of any point on the wall surface with
respect to a reference z-axis (assumed to be vertical).

g is the gravitational constant

ΔP_1 is the pressure difference of the glass between its O.D. and I.D.
surfaces

r is the inside radius of the glass tubing

Appendix 5

State of Art in Optical-fiber Transmission

In this Appendix, the current state of art in the field of optical-fiber transmission is briefly summarized. Assistance was generously contributed by private communications from the following persons, who are the world renowned leaders in this field. They include:

Professor W. A. Gambling, University of Southampton, England

Dr. Ting-ye Li, Bell Telephone Lab - Crawford Hill

Dr. Enrique A. J. Marcatili, BTL - Crawford Hill

Dr. Detlef Gloge, BTL - Crawford Hill

Dr. Dietrich Marcuse, BTL - Crawford Hill

Dr. John Williams, BTL - Crawford Hill

Dr. Peter C. Schultz, Corning

Dr. Peter L. Mattern, Sandia - Livermore

It is to be emphasized that any errors which may exist in this Appendix are strictly my own, and not attributable to any of the above persons.

1. Optical-fiber transmission is a technology which will find application in the communications industry. Progress in optical-fiber transmission during rhe last few years has been so rapid and abundant that technical feasible optical-fiber transmission s-stems should be available to the communications industry in the near future.

2. Optical-fiber transmission excels over other optical transmission means such as light piping, and lens system. In the latter two methods, turbulence and temperature gradients in the atmosphere can cause the propagating beam to be feflected. For example, a collimated beam of 5 cm. diameter at visible wavelengths is deflected by a transverse temperature of only a few thousandths of a degree, over a distance of 1.5 km, through a distance equal to 5 cm. Also, the earth movements

can introduce distottions. Although the thermal gradients in the atmosphere can be solved by the evacuation of gases from the light pipe, and the earth movements can be automatically corrected, these corrective measures invariably increase not only the installation costs but also the maintenance costs as well. Consequently, optical fiber transmission offers the real solution to the communication demands.

3. There are two basic requirements to a realistic transmission medium. They are:

(i) low transmission loss (attenuation):

Transmitter (T) of light through an optical fiber is given by:

$$T = I/I_o = p (1 - r)^2 \exp (-\alpha x)$$

(5-1)

Where I - transmitted light intensity

I_o = incident light intensity

p = parking factor

$r = (n-1)^2/(n+1)^2$

= Fresnel reflection at bundle end face (air-glass)

α = total attenuation coefficient in cm^{-1}

n = core index of refraction

x = length of fiber in cm

Attenuation α' can be expressed in unit of dB, which is given as $10 \log (I_o/I)$. Power loss is usually expressed as attenuation per unit fiber length (dB/km). In Table 5-1, a list of α, α', and T values is given to aid the easy comprehension of the conversions between these values.

(ii) low dispersion:

The dispersion is the change in group velocity (V_g) with respect to frequency ω. Over a long length of fiber, the dispersion causes the components of a modulated carrier separated in time and distortion occurs. In a single mode fiber, dispersion is only limited to that caused by the bulk glass and the surface wave (HE_{11}) mode. The low dispersion corresponds to a high pulse rate or bandwidths of several gigahertz $(10^9$ Hz) over several kilometers. In a multimode fiber, the lowest dispersion value of 0.3 ns $(10^{-9}$ sec) corresponds to a bandwidth of only 100 MHz over 1 km.

4.   In terms of material parameters, the above two requirements are being met by the following ways:

(i) loss due to material inhomogeneity scattering:

Scattering loss due to material inhomogeneities such as density and concentration fluctuations frozen in the glass is less than 1 dB/km at 1.0 μm wavelength. Imperfections such as bubbles and foreign particles produce very large losses. For instance, 1 ppm of platinum particles with 1 μm size gives a loss of 900 dB/km. Inhomogeneity is the boundary between the cladding and the core, and bending of the fiber can contribute an attenuation of about 1-2 dB/km.

(ii) loss due to glass material (Rayleigh scattering):

Rayleigh scattering is associated with scattering centers much smaller than one wavelength (λ) diameter and is proportional to λ^{-4}. The Rayleigh scattering loss is a function of the glass composition. Up to about 10 months ago, fused silica glass was considered to have the lowest Rayleigh scattering loss. Recently,

TABLE 5-1

Conversions between α, α', and T

α attenuation coefficient cm^{-1}	α' $\dfrac{dB}{km}$	T transmission % (in 1 km length fiber, $p(1-r)^2$ assumed to be 1)
2.30×10^{-3}	1000	1×10^{-97}
2.0×10^{-3}	868.6	1.38×10^{-85}
2.30×10^{-4}	100	9.96×10^{-9}
2.0×10^{-4}	86.9	2.0×10^{-7}
1.15×10^{-4}	50	9.98×10^{-4}
4.606×10^{-5}	20	0.999
2.303×10^{-5}	10	9.996
2.0×10^{-5}	8.6	13.53
1.15×10^{-5}	5.0	31.62
2.303×10^{-6}	1.0	79.43
2.0×10^{-6}	0.87	81.87
1.152×10^{-6}	0.5	89.12
2.303×10^{-7}	0.1	97.72
2.0×10^{-7}	0.087	98.02
2.303×10^{-8}	0.01	99.77
2.0×10^{-8}	0.0087	99.80

some binary component glasses were found to have lower Rayleigh scattering loss than high purity fused silica glass. This issue is not yet fully resolved due to impurity contents which are invariably present.

(iii) loss due to impurities:

The impurity loss is a major source of loss. The impurity ions, responsible for absorption in the near infrared wavelength region where optical sources are readily available are the transition-metal ions such as Ni^{2+}, Cu^{2+}, Fe^{2+}, Co^{2+}, Cr^{3+}, V^{3+}, Mn^{3+}, and Fe^{3+} and the hydroxyl ion OH^-. Loss contribution from each of the transition-metal ions is less than 1 dB/km for a concentration of 1 ppb, and that from the hydroxyl ion is about 1 dB/km for a concentration of 1 ppm.

(iv) dispersion due to material:

The refractive index of glass is not a linear function of frequency. The resulting delay spread is proportional to the spectral width of the optical signal. For silica glass, the dispersion is approximately 1 ns/km for a bandwidth of 1% in the wavelength region 0.8-0.9 μm, and about half of that in the region 1.0-1.1 μm.

(v) dispersion due to the waveguide effect:

The multimode delay spread of an ideal fiber of uniform index profile is given by

$$\tau_u = n\ \Delta L/c \qquad (5\text{-}2)$$

where n is the index of the core, Δ is the relative index difference between the core and the cladding, L is the fiber length, and c is the velocity of light in vacuum. A fiber with $\Delta = 0.01$ shows a large specific

delay spread of $\tau_{u/L} = 50$ ns/km. There are two simple ways to reduce this dispersion effectively.

(a) Graded index profile in the fiber core:

The profile of the refractive index of the fiber core can be graded to produce nearly equalization of the group velocities of the different modes. A parabolic distribution is the most effective profile. For example, the delay spread of a fiber of parabolic profile is given by

$$\tau_p = n\,\Delta^2 L/2c \tag{5-3}$$

which is smaller than τ_u by a factor of $\Delta/2$.

(b) Mode coupling:

Coupling among modes causes the power in a propagating pulse transfers from mode to mode and arrives at the output end with a propagation delay that is averaged over all modes. Actual coupling mechanism can be either index variations or geometry variations along the longitudinal direction. Mode coupling reduces multimode delay spread by a factor of $\sqrt{L/\ell_c}$, where L is the fiber length and ℓ_c is the coupling length.

5. State of art about the manufacturing methods of the optical fiber:

(i) Majority (over 95%) of the optical fiber has a glass core and a cladding which is usually glass. In special cases, plastic cladding has been used.

(ii) Majority (over 95%) of the optical fiber is made from glass preform. A glass preform consists of an inner glass rod and a glass tubular envelope. In most current practices, the glass preform is evacuated and is sealed.

(iii) Some of the glass rods, used to make preform, are made in the conventional glass rod fashion. Currently, the best high purity low loss, glass rods

are made first by the chemical vapor deposition (flame pyrolysis) method ("soot" process as developed by Corning) and a subsequent heat treatment to shrink the "soot" to a clear, optical quality, rod. There are variations to this method, mostly in terms of the heating source used in the CVD (flame pyrolysis) process.

(iv) Currently, the graded parabolic index of refraction profile is accomplished during the CVD (flame pyrolysis) process with concurrent dopants deposition.

6. State of art about the glass composition:

(i) Basically, the glass core composition starts with a fused silica glass with doping of Ti or Ge to increase the refractive index of the core.

(ii) Recently, binary glass compositions such as Na_2O-SiO_2 and K_2O-SiO_2 have also been used.

7. A study, conducted by Dr. Peter L. Mattern and his colleagues at Sandia Laboratories - Livermore, on the effects of radiation on the absorption and luminescence of fiber optic wave guides and materials (report issued July 1974) produced extremely important results which may have far-reaching implications. Their study showed that the Corning 7971 Ti-silicate glass exhibited several-fold higher sensitivity to radiation than the Schott fibers with Suprasil core. This sensitivity to radiation would place a limitation to the length of fiber. While there are insufficient data to relate high dosage, short time, radiation effect to the low dosage, long time, radiation effect, the results of Mattern's study raise serious question to the doped fused silica glass composition. This aspect must await further study. It appears that intrinsic glass compositions such as Na_2O-SiO_2 may have better radiation-resistant properties than the doped fused silica compositions.

References

1. W. E. Langlois, "Slow Viscous Flow", MacMillan Co., N. Y. (1964) p.112

2. L. A. Slobozhanin, "Equilibrium Shapes of Rotating Liquid Surface at Zero-G", Fluid Dynamics, $\underline{1}$, (5), 113-6 (1966).

3. Robert C. Paule, "Calculation of Complex Equilibria Involving Vaporization with Vacuum", Inorganic Chemistry Section, NBS, NASA Contract W-13, 475 #3, (June 4, 1974).

4. T. G. Wang, M. M. Saffren, and D. D. Elleman, "Acoustic Chamber for Weightless Positioning", paper presented at AIAA 12th Aerospace Science Meeting, Washington, D. C. Jan. 30 - Feb. 1, 1974

5. D. Kloepper and R. H. Will, "Boron Filament Manufacture in Space - A Literature Feasibility Study", NASA - ME-69-1, "Space Processing and Manufacturing", (October 1, 1969), p. 79.

6. M. G. Chernyak et al, "A Method of Calculating the Diameter of a Continuous Glass Filament", Glass and Ceramics $\underline{15}$, (1958) 639-43.

7. M. G. Chernyak, S. S. Kutukov, and B. I. Baskov, "Producing Continuous Glass Fiber with a High Hydrostatic Pressure in the Molten Glass", Glass and Ceramics $\underline{26}$, (1966) 27-30.

8. S. S. Kutukov and M. D. Khodakovskii, "Investigating the Movement of Glass in the Forming of Continuous Glass Fiber by High Speed Filming", Glass and Ceramics $\underline{24}$, 63-70 (1964).

9. Philomena G. Grodzka, "Gravity-Driven and Surface Tension-Driven Convection in Single Crystal Growth", NASA-ME-69-1, "Space Processing and Manufacturing" (October 21, 1969) p. 434.

10. E. Fromm and H. Jehn, "Electromagnetic Forces and Power Absorption in Levitation Melting", Brit. J. Appl. Phys., $\underline{16}$, 653-63 (1965).

11. P. L. Mattern, "A Summary of Preliminary Studies on the Effects of ^{60}Co Gamma-Ray Irradiation of Fiber Optic Materials", Sandia Lab. report SLL-73-0287, (October 1973).

12. P. L. Mattern, L. M. Watkins, C. D. Skoog, J. R. Brandon, E. H. Barsis, "Effects of Radiation on the Absorption and Luminescence of Fiber Optic Waveguides and Materials", Sandia Lab. report SAND 74-8622, (July 1974).

13. E. J. Friebele, R. J. Ginther, and G. H. Sigel, Jr., "Radiation Protection of Fiber Optic Materials: Effects of Oxidation and Reduction", Appl. Phys. Lett. $\underline{24}$ (9), 412 (1974).

14. Harold L. Schick, "Thermodynamics of Certain Refractory Compounds", Academic Press, N. Y. (1966) vols. I and II.

15. W.E. Langlois, "Slow Viscous Flow", MacMillan Co., N.Y. (1964) p. 112.

16. R.L. Ketter and P.P. Prawel, "Modern Methods of Engineering Computation", McGraw-Hill, N.Y. (1969) p. 278.

17. H.F. Bauer and J. Siekmann, "On the Shape of a Rotating Fluid System Consisting of a Gas Bubble Enclosed in a Liquid Globe", ZAMP, $\underline{22}$, 532-42 (1971).